Mechanism of diffusion in the smectic-*A* phase of wormlike rods studied by computer simulation

Giorgio Cinacchi*
Centro di Ricerca "Ercole De Castro," Università di Bologna, Via Vincenzo Toffano 2, I-40125 Bologna, Italy

Luca De Gaetani†
Dipartimento di Chimica, Università di Pisa, Via Risorgimento 35, I-56126 Pisa, Italy

(Received 25 July 2008; revised manuscript received 14 October 2008; published 20 January 2009)

Molecular dynamics computer simulations have been carried out in the smectic-*A* phase of stiff wormlike rods. The analysis of the long trajectories generated has allowed for a detailed insight into that diffusion mechanism which is operative in the above-mentioned liquid-crystalline phase, as recently visualized in a system of colloidal virus rods. Fast particles, i.e., those able to move abruptly out from one into an adjacent layer, have been identified. Their properties, such as the velocity autocorrelation function and the orientational distribution function, have been determined and compared to the corresponding quantities valid for a generic rod.

DOI: 10.1103/PhysRevE.79.011706 PACS number(s): 61.30.St, 66.10.cg

Smectic-*A* (S_A) liquid crystals are complex fluids characterized by a layered structure. While moving, the constituent particles tend to not only maintain, as in the nematic phase, their principal axis along a preferred direction, the director ($\hat{\mathbf{n}}$), but also reside within a layer, the normal of which coincides with $\hat{\mathbf{n}}$ [1]. Particle diffusion in S_A phases was already addressed in computational and experimental papers (e.g., Refs. [2–8]). These papers reported on the value of the diffusion coefficients parallel ($D_\parallel$) and perpendicular ($D_\perp$) to the director, their temperature dependence, as well as the role that the rare interlayer transverse particles might have in the interlayer diffusion [3], all recognizing that the motion of the particles through the layers shows distinct characteristics with respect to that within the layers. However, not one of these studies addressed the peculiar mechanism by which the particles move through the layers, which received the name of permeation [9].

One account on the permeation process at the single particle level has been recently presented in Ref. [10], where a system of *fd* virus particles in their S_A phase [11] has been investigated. Certain of these stiff rodlike particles have been labeled with a fluorescent dye, so that their individual motion in the S_A environment formed by the other unlabeled *fd* particles could be directly visualized by fluorescence video microscopy. It has been observed that the diffusion through the layers of these colloidal rods occurs via discrete jumps of one particle length. Since the positions of the labeled rods could be monitored, the mean-field layering potential energy (U_{layer}) and the mean-square displacements (MSDs) parallel and perpendicular to the director in both the nematic and smectic-*A* phases have been also determined. Interestingly, U_{layer} has been found to be sinusoidal, thus giving further confirmation of this assumption, frequently adopted in the theoretical calculations on the S_A phase (e.g., Ref. [12]). Equally of interest is the observation that $D_\parallel$ in the S_A phase can be given in terms of the diffusion coefficient along the director in the nematic phase multiplied by a factor depending on U_{layer}, thus corroborating, to a certain extent, this sort of assumption made in the analysis of experimental diffusion data in the S_A phase [8]. While the motion perpendicular to $\hat{\mathbf{n}}$ has been always found strongly subdiffusive in both the nematic and smectic-*A* phases, irrespective of the value of the ionic strength, the motion parallel to $\hat{\mathbf{n}}$ has been found diffusive in the nematic phase and in the smectic-*A* phase at high ionic strength but moderately subdiffusive in the smectic-*A* phase at low ionic strength.

With the intention of being a hopefully useful complement to the experiments of Ref. [10], the present work investigates the permeation process in the S_A of model wormlike rods via molecular dynamics (MD) computer simulations [13].

The model particles, of mass m, are of the same type employed previously [12,14–16]. Each of them consists of nine beads. Two contiguous beads are maintained at a fixed distance of 0.6σ, with σ the unit of length. The particle length, ℓ, is thus $\simeq 5.8\sigma$. Harmonic bending interactions, v_{lmn}, of the type

$$v_{lmn} = \tfrac{1}{2}K(\theta - \pi)^2, \tag{1}$$

with θ the angle formed by the lm and mn bonds and K the relevant constant, regulate the stiffness of the beadlace rod. Between two beads, i and j, belonging to either the same particle or two different particles, the following truncated and shifted Lennard-Jones interaction applies:

$$u_{ij}(r) = \begin{cases} 4\epsilon\left[\left(\dfrac{\sigma}{r}\right)^{12} - \left(\dfrac{\sigma}{r}\right)^{6} + \dfrac{1}{4}\right], & r \leqslant 2^{1/6}\sigma, \\ 0, & r > 2^{1/6}\sigma, \end{cases} \tag{2}$$

with ϵ the unit of energy. The complete phase behavior of these wormlike rods has been recently traced as a function of K [16]. In the present work, K has been set to 5555ϵ, a value sufficiently large to ensure the existence of a S_A phase [16].

One well-equilibrated S_A configuration of 600 of such wormlike rods, taken from one of the previous MD runs [17], has been chosen to start an equilibration run in the

*g.cinacchi@sns.it
†degaetani@dcci.unipi.it

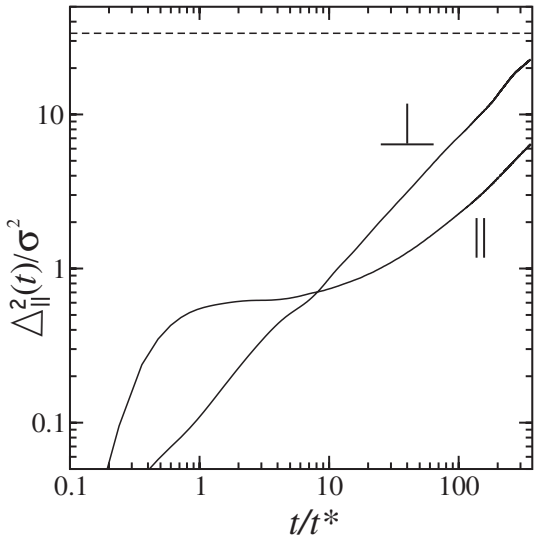

FIG. 1. Mean-square displacements parallel (∥) and perpendicular (⊥) to the director. The dashed line indicates the value of ℓ^2.

microcanonical ensemble [13]. This run has lasted 10^7 time steps, the duration of each time step having been $1.09 \times 10^{-4} t^*$, with $t^* = (\frac{m}{\epsilon})^{1/2}\sigma$ the unit of time. The equilibration run has been then followed by two production runs, still in the microcanonical ensemble. During the first, of 10^7 time steps, the positions of the nine beads of all the wormlike rods have been saved every 55 time steps and stored in a file for the subsequent analysis. During the second, of 4×10^6 time steps, the velocities of the nine beads of all the wormlike rods have been saved every 35 time steps and stored in a file for the subsequent analysis.

From the temporal evolution of the center of mass of each wormlike rod, the MSD parallel ($\triangle_{\parallel}^2$) and perpendicular ($\triangle_{\perp}^2$) to the director have been computed according to the formulas

$$\triangle_{\parallel}^2(t) = \langle [\mathbf{r}(t+\tau)\cdot\hat{\mathbf{n}}(\tau) - \mathbf{r}(\tau)\cdot\hat{\mathbf{n}}(\tau)]^2 \rangle,$$

$$\triangle_{\perp}^2(t) = \langle [\mathbf{r}(t+\tau)\times\hat{\mathbf{n}}(\tau) - \mathbf{r}(\tau)\times\hat{\mathbf{n}}(\tau)]^2 \rangle, \qquad (3)$$

where $\mathbf{r}(t)$ and $\hat{\mathbf{n}}(t)$ are, respectively, the center-of-mass position and director at time t and $\langle\cdots\rangle$ signifies a statistical average over particles and time origins τ. Parallel and perpendicular diffusion coefficients $D_{\parallel}$ and $D_{\perp}$ have been calculated by the long time limit of MSDs through the standard Einstein relation. Figure 1 shows the two MSDs. Three distinct regimes can be noticed. The parallel MSD is larger than the perpendicular MSD at short times. This is expected on the basis of the rodlike character of the particles; in the nematic phase, this behavior persists at long times (e.g., Refs. [14,18,19]). The specific nature of the S_A phase emerges at intermediate times. The presence of layers exerts a barrier over the motion along the director and the parallel MSD significantly reduces its slope to such an extent that, around $5t^*$, the values of the two MSDs approach and become very similar. Concomitantly, also the $\triangle_{\perp}^2$ shows a decrease, which is, however, very gentle and of short duration. The relatively high value of the plateau in the $\triangle_{\parallel}^2$ is due to the particle oscillations around the equilibrium position within a layer; notwithstanding the high packing of the S_A phase, the amplitude of these oscillations is $\sim 0.8\sigma$, i.e., $\sim 15\%$ of the particle length. Then, at longer times, after the exchange of the values of the two MSDs has occurred, the $\triangle_{\perp}^2$ grows faster than the $\triangle_{\parallel}^2$. The two MSDs reach a linear behavior on a different time scale, after approximately $100t^*$ and $10t^*$ for $\triangle_{\parallel}^2$ and $\triangle_{\perp}^2$, respectively. When both have reached the diffusive behavior, the values of the diffusion coefficients result to be $D_{\parallel} = 0.008\sigma^2 t^{*-1}$ and $D_{\perp} = 0.034\sigma^2 t^{*-1}$. The diffusion coefficient perpendicular to $\hat{\mathbf{n}}$ is larger than the one parallel to $\hat{\mathbf{n}}$. This fact is not new, particularly in the case of thermotropic smectogenic liquid crystals (e.g., Ref. [8]). It contrasts with the anisotropy of diffusion coefficients reported in Ref. [10], where it has been found that $D_{\parallel}$ for the *fd* colloidal rods is much larger than $D_{\perp}$. The experimental result of Ref. [10] is anyway reconcilable with previous and present data if one takes into account that the shape anisotropy of the experimental colloidal particles is much larger than that typical of thermotropic mesogenic molecules as well as that of the present model particles.

Being purely repulsive but without electrostatic charges, the latter cannot clearly rationalize the difference in the characteristics of MSD found in Ref. [10] by varying the ionic strength, nor appear able to reproduce the significant subdiffusive behavior of the $\triangle_{\perp}^2$ observed in these experiments. Nevertheless, purely repulsive models are known to be able to account for many of the structural and dynamical properties of lyotropic liquid crystals. Therefore, it is of interest to investigate whether the permeation process observed in the experiment is also operative in the S_A phase formed by the elementary wormlike rods.

Presumably, this should be the case. Besides potentially confirming this, computer simulation offers the additional possibility to individuate the particles able to move across two layers and determine their characteristics, which can then be compared to the respective counterparts valid for generic particles, not able to perform such a move, thus providing pieces of information perhaps not readily accessible by experiments.

To these ends, it has seemed more convenient to commence by analyzing the mean linear displacement (MLD), rather than the MSD, along the director. $\triangle_{\parallel}$ is defined in analogy with Eq. (3),

$$\triangle_{\parallel}(t) = \langle |\mathbf{r}(t+\tau)\cdot\hat{\mathbf{n}}(\tau) - \mathbf{r}(\tau)\cdot\hat{\mathbf{n}}(\tau)| \rangle. \qquad (4)$$

The distribution function pertinent to $\triangle_{\parallel}$ is $\Pi_{\parallel}(z(t))$. This distribution function is normalized to unity every time t. Thus, $\Pi_{\parallel}(z(t))dz$ represents the fraction of rods having traveled a distance comprised between z and $z+dz$ along $\hat{\mathbf{n}}$ in a time t. For $t=0$, this distribution function is a δ function. In the limit of $t\to\infty$, $\Pi_{\parallel}$ becomes the equilibrium, undulated, single-particle distribution function which is the characteristic of a S_A phase. The evolution of $\Pi_{\parallel}$ from $t=0$ toward the equilibrium limit can be appreciated in Fig. 2. Twelve curves are shown: The first from the top, having the highest peak at $z=0$, corresponds to $t=11.424t^*$; every successive curve corresponds to a time t which is 1.5 larger than the time corre-

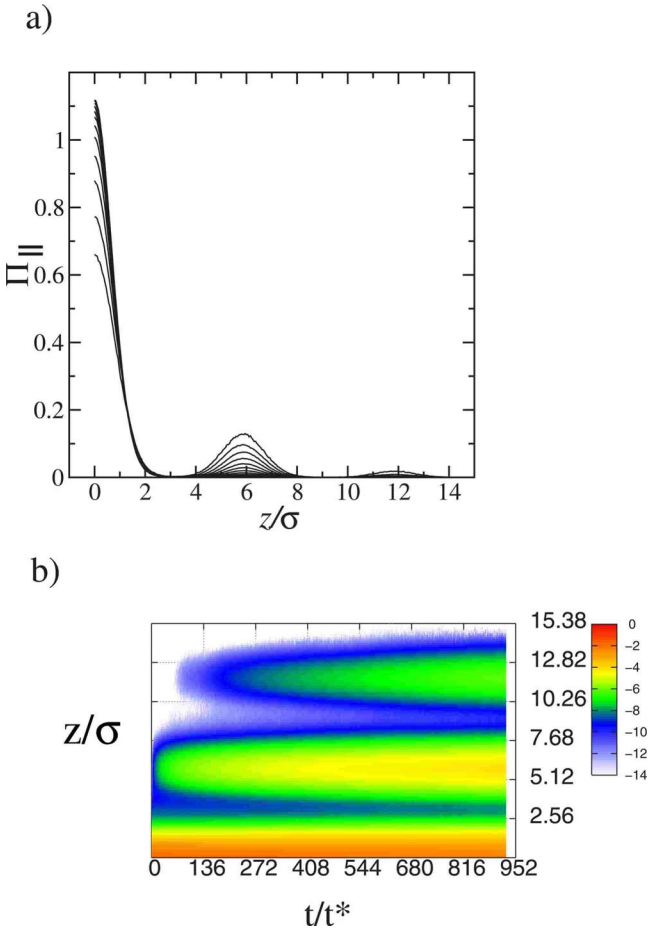

FIG. 2. (Color online) (a) $\Pi_{\|}(z(t))$: Distribution functions of a linear displacement along the director, z, at different intervals of time t. The first from the top, having the highest peak at $z=0$, corresponds to $t=11.424t^*$; every successive curve corresponds to a time t which is 1.5 larger than the time corresponding to the previous curve; the last curve shown corresponds to a $t=(1.5^{11})\times 11.424t^*=988.148t^*$. (b) Contour plot of $\Pi_{\|}(z(t))$.

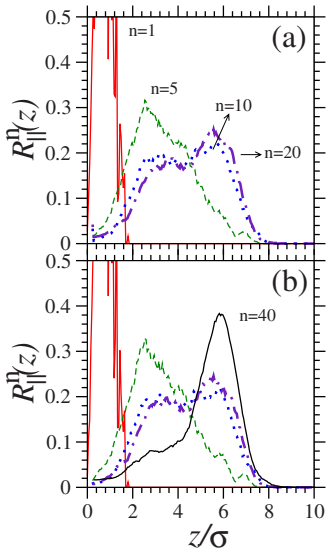

FIG. 3. (Color online) (a) $R^n_{\|}(z)$ for t_1: Distribution functions of a linear displacement along the director, z, for fast particles at several intervals of time $n\Delta t$, $\Delta t=0.18t^*$; $n=1$ (red), $n=5$ (green), $n=10$ (blue), $n=20$ (indigo). Next to each line is reported the corresponding number. (b) $R^n_{\|}(z)$ for t_2: Distribution functions of a linear displacement along the director, z, for fast particles at several intervals of time $n\Delta t$, $\Delta t=0.18t^*$; $n=1$ (red), $n=5$ (green), $n=10$ (blue), $n=20$ (indigo), $n=40$ (black). The colors-numbers correspondence is the same as in panel (a); moreover, the $n=40$ line is also indicated.

sponding to the previous curve. Thus, the last curve shown corresponds to a time $t=(1.5^{11})\times 11.424t^*=988.148t^*$. With the increase of t, the peak at $z=0$ naturally decreases. Concomitantly, a second peak at a value of z approximately equal to ℓ starts and then grows. For the largest values of t, a third peak at z approximately equal to 2 times the particle length, $\lesssim 12\sigma$, starts to be noticeable. During this process, the values of z approximately equal to one-half the particle length always exhibit a negligible probability density. This fact may be taken as a first indication that the evolution of $\Pi_{\|}$ could be determined by a jumplike mechanism. In fact, if particles slide one with respect to the other, staying a relatively considerable amount of time in the interlayer region, those corresponding values of z would have a non-negligible probability density.

One ulterior proof of the operativeness of a mechanism of this type can be achieved by identifying those fast wormlike rods that rapidly move out from one into an adjacent layer. The identification protocol has been the following. First, two large time intervals, $t_1=70.86t^*$ and $t_2=239.36t^*$, have been defined. Then, the trajectories of all the wormlike rods in these time intervals have been scrutinized; if a particle has moved along the director of a quantity J larger than 4.1σ, it is selected and labeled "passed," and the time at which this occurs is labeled t_J. The quantity J has been appropriately chosen to lay in the tiny population range of $\Pi_{\|}$ and close to the interlayer distance, $\sim\ell$; in Fig. 2, the abscissa 4.1σ corresponds to the incipience of the second peak, i.e., refers to a particle approaching the next layer.

The dynamics of each of these "passed" particles has been followed in the periods $n\Delta t$, with n a positive integer and $\Delta t=0.18t^*$, preceding the registration of the above-defined movement J, and the distribution functions, $R^n_{\|}(z)$, of the rod displacements along the director in these periods of time, $z=|\mathbf{r}(t_J)\cdot\hat{\mathbf{n}}(t_J)-\mathbf{r}(t_J-n\Delta t)\cdot\hat{\mathbf{n}}(t_J)|$, constructed. These distribution functions are all normalized to unity. They are plotted in Fig. 3 for $n=1,5,10,20$ and t_1 in panel (a), and for $n=1,5,10,20,40$ and t_2 in panel (b). Once having reversed the time arrow, the fraction of the "passed" particles, p_n, is then given by

$$p_n=\int_J^\infty dz R^n_{\|}(z). \tag{5}$$

One can notice that the distribution function for $n=1$ is centered about 1, that is, all the displacements are within a layer, and the corresponding value of p_1 is 0. Then, on increasing n, the form of the distribution function rapidly changes, becoming broader; the abscissa of its peak moves toward larger values. For $n=10$ already, the distribution function shows a plateau extending from $z\sim 2$ to $z\sim\ell$. For $n=20$, the abscissa

of the peak has already reached the value of ℓ, but the distribution function is still broad. For $n=40$, apart from a residual, modest tail at smaller values of z, the distribution function is well peaked around the abscissa corresponding to one rod length. These changes in the form of the distribution functions are accompanied by the corresponding increase in the value of p_n, 0.28 for $n=5$, 0.55 for $n=10$, 0.60 for $n=20$, and 0.79 for $n=40$. These numbers, together with the form of the parent distribution functions, indicate that the majority of "passed" wormlike rods completes the passage from one layer to another in a very short amount of time: For example, at least 50% of particles have passed in $10\Delta t$, i.e., $1.8t^*$. In fact, the distribution functions of Fig. 3 are insensitive to the time window t_1 or t_2; the shortest between these two time intervals, t_1, is already sufficiently long to observe the phenomenon. From Fig. 2, it is clear that the vast majority of particles keeps staying in one layer for a considerable amount of time: The peak at 0 in the panel (a) of that figure is the highest for all curves shown. For example, the percentage of particles succeeding in the passage to one of the adjacent layers over all the particles of the sample is approximately 8% after a time interval of $130t^*$ has elapsed. These successful wormlike rods have nevertheless passed in a very short period of time, confirming that permeation is a rare and sudden event.

Having individualized the fast particles, it is of interest to investigate whether these particles have peculiar characteristics.

First, the velocity of the "passed" particles is focused on. In analogy with what was done for the identification of the "passed" wormlike rods, three intervals of time are defined, t_{v1}, t_{v2}, and t_{v3}, whose duration is, respectively, $23.66t^*$, $35.50t^*$, and $53.31t^*$. Within these periods of time, the trajectories of the particles are controlled and those particles which have traveled more than J are identified. The instant at which this happens is registered as t_J. One can define the autocorrelation function of the velocity parallel to the director as

$$C_{\parallel}^{vv}(t) = \langle [\boldsymbol{v}(t+\tau)\cdot\hat{\mathbf{n}}(\tau)][\boldsymbol{v}(\tau)\cdot\hat{\mathbf{n}}(\tau)]\rangle, \tag{6}$$

with $v(t)$ the center-of-mass velocity of a particle at time t. The $C_{\parallel}^{vv}(t)$ is computed for the "passed" particles for the period of time of $600\Delta t_v$, with $\Delta t_v = 7.6\times 10^{-3}t^*$, preceding t_J. $C_{\parallel}^{vv}(t)$ is also computed for all the wormlike particles. The velocity autocorrelation functions concerning the fast rods as well as the completely averaged velocity autocorrelation function are displayed in Fig. 4. One can notice that all velocity autocorrelation curves start at $t=0$ with the same value, i.e., $\sqrt{k_BT/m}$. Initially, even those rods which are so fast to pass from one layer to another do not have a velocity higher than that of the other rods. What makes these particles fast is experienced at successive times. The $C_{\parallel}^{vv}(t)$ of the fast particles has a less negative rebound at approximately $0.2t^*$. The faster the particle is, i.e., it is able to move across two layers in a time at most equal to t_{v1} rather than t_{v3} or t_{v2}, the less deep is the negative lobe of the velocity autocorrelation function. In fact, the depth of the negative lobe of the curve corresponding to a time interval t_{v1} is lower than that of the negative lobe of the curve corresponding to a time interval t_{v2}, and a similar comment applies to the pair of curves corresponding to time intervals t_{v2} and t_{v3}. In addition, examining the tail of these functions at a time approximately equal to t^*, one can notice that, while the completely averaged $C_{\parallel}^{vv}(t)$ is still negative, the $C_{\parallel}^{vv}(t)$ for the fast particles is less negative or even positive. This means that, at $t\simeq t^*$, while a generic rod tends to move in a direction opposite to the one it had at $t=0$, a fast rod may even continue to proceed along the initial direction. The differences between a generic rod and a fast rod are well appreciated observing the integrals of the velocity autocorrelation functions, $I_{\parallel}^{vv}(t)$. These functions all have an initial rapid increase, followed by a descent in correspondence of the negative lobe of $C_{\parallel}^{vv}(t)$. However, for $t\geqslant t^*$, while that corresponding to the completely averaged $C_{\parallel}^{vv}(t)$ keeps decreasing monotonically, those corresponding to the fast particles oscillate around a constant value or even increase in an oscillatory manner. This situation is reflected in the behavior of the $\triangle_{\parallel}^2$, which is the integral of the corresponding $I_{\parallel}^{vv}(t)$ and shown in the inset of Fig. 4. Two are the characteristics relevant to be noticed. The subdiffusive behavior corresponding to the plateau observable around $t\sim t^*$ and which characterizes the completely averaged $\triangle_{\parallel}^2$ is significantly reduced or even completely absent in the case of fast rods. In addition, the long time slope of the $\triangle_{\parallel}^2$'s for the fast rods is an order of magnitude larger than that of the completely averaged $\triangle_{\parallel}^2$. Those rods which are able to pass from one to an adjacent layer may be called "fast" not because they have an intrinsic larger velocity but because they casually experience more favorable collisions with the other wormlike rods. In this sense, rather than a jumplike mechanism, passing particles are characterized by a fortuitous chain of events, in which backward collisions are less frequent.

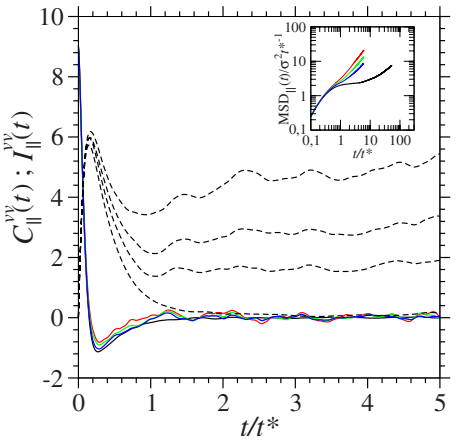

FIG. 4. (Color online) Velocity autocorrelation functions, $C_{\parallel}^{vv}(t)$: Completely averaged (black) and those for fast rods (blue, t_{v3}; green, t_{v2}; red, t_{v1}); integral of $C_{\parallel}^{vv}(t)$, $I_{\parallel}^{vv}(t)$, dashed lines. For clarity, the ordinate of the functions $I_{\parallel}^{vv}(t)$ are multiplied by 10. The lowest curve corresponds to completely averaged $C_{\parallel}^{vv}(t)$, while the successive curves to t_{v3}, t_{v2}, and t_{v1}, respectively, on increasing order. The inset shows the $\triangle_{\parallel}^2(t)$: Completely averaged (black) and those for fast rods (blue, t_{v3}; green, t_{v2}; red, t_{v1}).

In this regard, it is of interest to investigate whether these fast particles have peculiar orientational characteristics that might help them in receiving more favorable collisions from

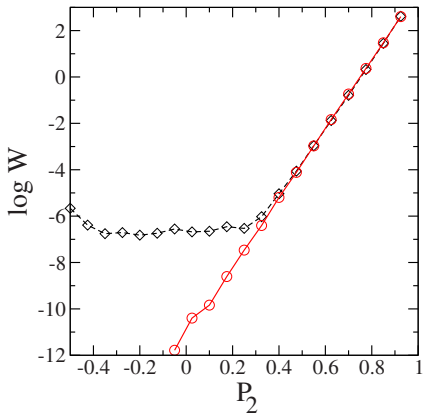

FIG. 5. (Color online) Distribution function, W, of P_2 for a generic rod (diamonds and black dashed line) and a fast rod (circles and red solid line).

the surroundings. The Monte Carlo simulation work of Ref. [3] already suggests that the very few particles which lay, perpendicularly to the director, in the interstices between two layers [20], have no role in the diffusion mechanism. The present Fig. 5 confirms this conclusion. In this figure, the probability distribution function, $W(P_2)$ of $P_2=\frac{3}{2}(\hat{\mathbf{u}}\cdot\hat{\mathbf{n}})^2-\frac{1}{2}$, with $\hat{\mathbf{u}}$ the principal axis of a rod, is depicted for both a generic rod and a fast particle. The probability density to be transverse, already very scanty for a generic rod, is more than so for fast particles. The latter are well aligned with the director during the passage. Not only transverse particles have no role in the diffusion mechanism, as observed in Ref. [3], but having a transverse orientation with respect to the director is even detrimental to the passage across smectic layers.

Having identified the fast particles and characterized their velocity autocorrelation function and orientational distribution function, it is of interest to investigate how long the condition of being "fast" persists.

Figure 6 illustrates the probability density for a particle to travel a distance $r_{\parallel,12}$ along the director in the time interval $[s;2s]$, with $s=350t^*$, known that it has traveled for a distance $r_{\parallel,01}$ along the director in the time interval $[0:s]$. The

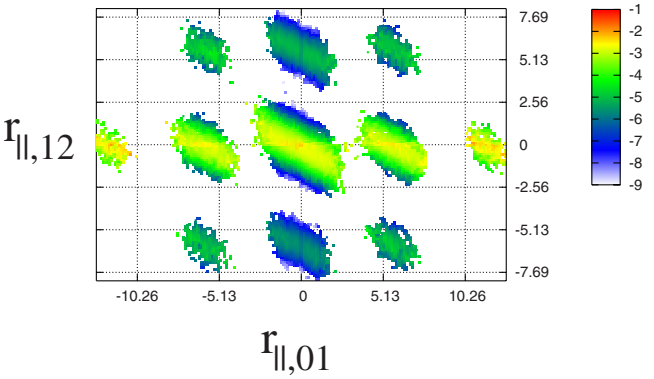

FIG. 6. (Color online) Probability density map for a particle to travel a distance $r_{\parallel,12}$ along the director in the time interval $[s;2s]$, known that it has traveled for a distance $r_{\parallel,01}$ along the director in the time interval $[0:s]$.

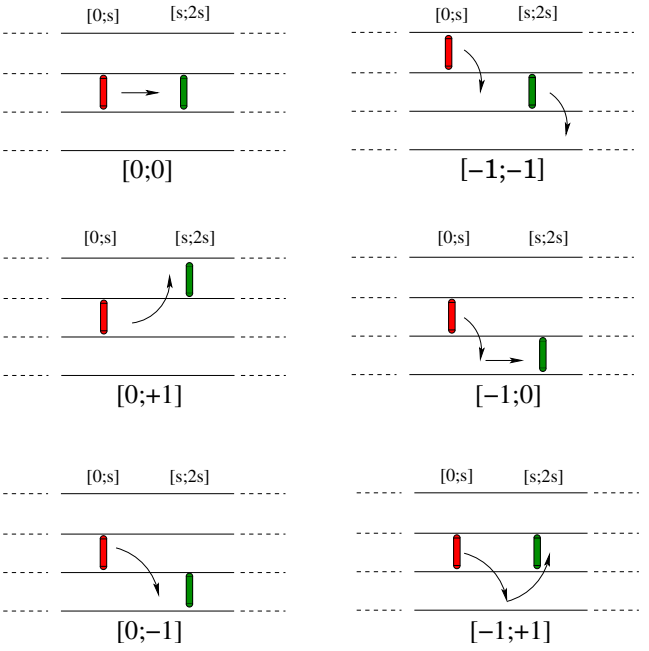

FIG. 7. (Color online) Schematic illustration of the various movements relevant to Fig. 6. $\pm\ell$ indicates movements of circa one particle length across the layers.

spots of this figure are separated by approximately 1 particle length while moving in both directions of abscissa and ordinate. One passage from one to a contiguous layer corresponds to $(r_{\parallel,01},r_{\parallel,12})=(0,|\ell|)$ or $(|\ell|,0)$, while two subsequent passages to $(|\ell|,|\ell|)$. The normalization of this probability density has been carried out such that, for every abscissa value, the integration over the ordinate values gives 1. This choice makes the population corresponding to $r_{\parallel,01}=k\ell$, with k a nonzero integer, quantitatively comparable with the population corresponding to $r_{\parallel,01}=0$. Without this type of normalization, the probability density at $r_{\parallel,01}=k\ell$ would be much lower than that at $r_{\parallel,01}=0$, since the passages are rare. The particles that have traveled in the first time interval $[0:s]$ of a quantity $\sim k\ell$ are thus the "fast" particles, while those corresponding to $r_{\parallel,01}=0$ have resided in a layer during the first period. The latter may either continue to reside in the same layer $[(r_{\parallel,01},r_{\parallel,12})=(0,0)]$ or move to a contiguous layer $[(r_{\parallel,01},r_{\parallel,12})=(0,|\ell|)]$, in the period $[s;2s]$, while those rods that have been fast in the first time interval may retain $[(r_{\parallel,01},r_{\parallel,12})=(|\ell|,|\ell|)]$ or remit $[(r_{\parallel,01},r_{\parallel,12})=(|\ell|,0)]$ this condition. Figure 7 illustrates schematically these considerations.

The fact that the chain of spots corresponding to $r_{\parallel,01}=k\ell$ shows essentially the same probability density values than that corresponding to $r_{\parallel,01}=0$ demonstrates that the casually acquired condition of being "fast" is generally not maintained for long. In fact, the probability density to pass from one to the adjacent layer in the time interval $[s;2s]$ is the same irrespective of the fact that the particle has succeeded or not to move through the layers in the previous interval $[0;s]$.

Moreover, no connection exists between the probability to pass and the distance a rod has traveled in a previous time interval. This is demonstrated in Fig. 8, where the probability

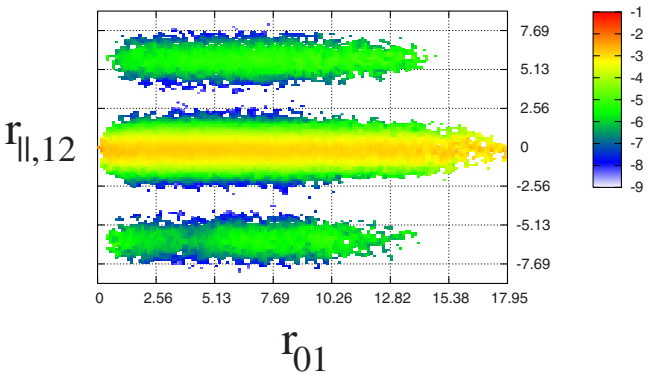

FIG. 8. (Color online) Probability density map for a particle to travel a distance $r_{\|,12}$ along the director in the time interval $[s;2s]$, known that it has traveled for a distance r_{01} in the time interval $[0:s]$.

density for a particle to travel a distance $r_{\|,12}$ along the director in the time interval $[s;2s]$, known that it has traveled for a distance r_{01} in the time interval $[0:s]$, is shown. No dependence of $r_{\|,12}$ on r_{01} is apparent. Only one wide spot is observed for $r_{\|,12}\sim 0$ or $r_{\|,12}\sim k\ell$.

The mechanism of passage of a rod from one to an adjacent layer has a number of characteristics in common with the motion of a particle in a supercooled fluid [21–23]. In both cases, a particle must escape from a cage; a mark of the occurring of this phenomenon is the subdiffusive intermediate behavior of MSD. In addition, in both systems, one can distinguish between "fast" or "mobile" particles and "generic" or "slow" particles. In supercooled fluids, clusters of mobile particles [21] and strong cooperative motion [22] have been observed, and the mobile particles collectively move from one metabasin to another, maintaining their condition for a long time [23]. In particular, a chainlike, collective, and cooperative mechanism was reported to be operative in supercooled fluids [22]. This type of mechanism is not *a priori* entirely incompatible with the structure of a smectic-*A* phase. In fact, one may imagine chains of rods moving across the smectic layers, as schematically depicted in Fig. 9.

If a mechanism of this kind were actually operative in the present smectic-*A* phase of wormlike rods, it would imply that the probability density of a passage in the period $[s;2s]$ would be larger for the case of a rod having also passed in the period $[0;s]$ in Fig. 6, as well as the probability density of a passage in the period $[s;2s]$ would have a maximum for $r_{01}\sim\ell$ in Fig. 8. The conjoint absence of the former feature in Fig. 6 and the latter feature in Fig. 8 seems to point to the conclusion that a chainlike mechanism, involving collections of rods moving cooperatively, is absent in the smectic-*A* phase studied in the present work. It would appear, instead, that fast rods individually execute the passages through the layers and they acquire the condition of being fast as suddenly as they lose this.

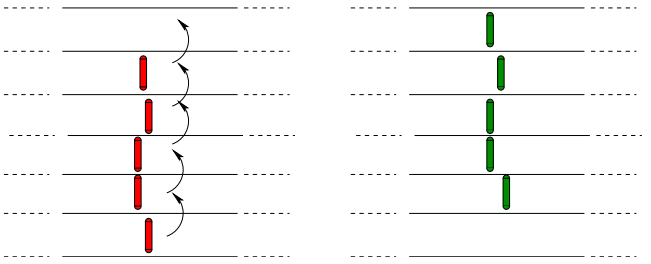

FIG. 9. (Color online) Schematic illustration of a possible chainlike diffusion mechanism across smectic layers.

In conclusion, the mechanism of diffusion in the smectic-*A* phase of stiff wormlike rods has been studied by molecular dynamics computer simulation. The present calculations reproduce the permeation behavior across the smectic layers experimentally observed in the smectic-*A* phase of colloidal *fd* virus rods [10]: Both model and real single particles move abruptly and rapidly from one to an adjacent layer. In addition, computer simulations have offered the possibility to analyze not only the trajectory of these fast rods but also their velocity autocorrelation function and orientational characteristics. From the latter point of view, it has been observed that the fast rods have a major tendency to be aligned along the director than generic rods. This fact seems to be, *prima facie*, in contrast to what was observed in a real colloidal sample formed by spherical particles, where it has been seen that those particles making large displacements are located in disordered regions [24]. This is expected in an isotropic fluid. The observation that, in a smectic-*A* phase, fast rods are more ordered than generic rods is nevertheless in accord with the known coupling between diffusivity and orientational order which exists in anisotropic fluids [25].

[1] P. Ostwald and P. Pieranski, *Smectic and Columnar Liquid Crystals* (CRC Press, Boca Raton, FL, 2005).
[2] D. Vaidya, D. A. Kofke, S. Tang, and G. T. Evans, Mol. Phys. **83**, 101 (1994).
[3] J. S. Van Duijneveldt and M. P. Allen, Mol. Phys. **90**, 243 (1997).
[4] G. T. Evans, D. S. Vaidya, and D. A. Kofke, Mol. Phys. **90**, 683 (1997).
[5] I. Furo and S. V. Dvinskikh, Magn. Reson. Chem. **40**, S3 (2002).
[6] Robin L. Blumberg Selinger, Phys. Rev. E **65**, 051702 (2002).
[7] M. A. Bates and G. R. Luckhurst, J. Chem. Phys. **120**, 394 (2004).
[8] M. Cifelli, G. Cinacchi, and L. De Gaetani, J. Chem. Phys. **125**, 164912 (2006).
[9] W. Helfrich, Phys. Rev. Lett. **23**, 372 (1969).
[10] M. P. Lettinga and E. Grelet, Phys. Rev. Lett. **99**, 197802 (2007).
[11] Z. Dogic and S. Fraden, Curr. Opin. Colloid Interface Sci. **11**, 47 (2006).
[12] G. Cinacchi, L. De Gaetani, and A. Tani, Phys. Rev. E **71**, 031703 (2005).

[13] J. M. Haile, *Molecular Dynamics Simulation: Elementary Methods* (Wiley, New York, 1997); D. C. Rapaport, *The Art of Molecular Dynamics Simulation* (Cambridge University Press, Cambridge, 2004).

[14] G. Cinacchi, L. De Gaetani, and A. Tani, J. Chem. Phys. **122**, 184513 (2005).

[15] D. Bertolini, G. Cinacchi, L. De Gaetani, and A. Tani, J. Phys. Chem. B **109**, 24480 (2005).

[16] G. Cinacchi and L. De Gaetani, Phys. Rev. E **77**, 051705 (2008).

[17] The 600 wormlike rods were placed in an orthorombic box, having six smectic layers, the normal of which coinciding, on average, with the z axis of the laboratory reference frame. The three sides of the computational box, L_x, L_y, L_z, were such that $L_x:L_y:L_z \approx 1:1:3$. The initial configuration was one generated during a previous isobaric-isothermal MD production run carried out at $P^*=P\frac{\sigma^3}{\epsilon}=24.716$ and $T^*=\frac{k_BT}{\epsilon}=8.63$. The packing fraction of the wormlike rods in this configuration was $\phi=\rho\sigma^3\frac{\pi}{6}(1+\frac{3\ell-\sigma}{2\sigma})=0.654$, i.e., the smectic-*A* phase is quite close to the transition to a phase with a hexagonal in-plane order [16].

[18] H. Löwen, Phys. Rev. E **59**, 1989 (1999).

[19] M. P. Lettinga, E. Barry, and Z. Dogic, Europhys. Lett. **71**, 692 (2005).

[20] R. van Roij, P. Bolhuis, B. Mulder, and D. Frenkel, Phys. Rev. E **52**, R1277 (1995).

[21] W. Kob, C. Donati, S. J. Plimpton, P. H. Poole, and S. C. Glotzer, Phys. Rev. Lett. **79**, 2827 (1997).

[22] C. Donati, J. F. Douglas, W. Kob, S. J. Plimpton, P. H. Poole, and S. C. Glotzer, Phys. Rev. Lett. **80**, 2338 (1998).

[23] G. A. Appignanesi, J. A. Rodriguez Fris, R. A. Montani, and W. Kob, Phys. Rev. Lett. **96**, 057801 (2006).

[24] E. R. Weeks and D. A. Weitz, Phys. Rev. Lett. **89**, 095704 (2002).

[25] M. P. Allen, Phys. Rev. Lett. **65**, 2881 (1990).